Chapter 1

LONG-TERM VARIATIONS IN THE GALACTIC ENVIRONMENT OF THE SUN

Nir J. Shaviv
Racah Institute of Physics, Hebrew University, Jerusalem 91904, Israel

Abstract We review the long-term variations in the galactic environment in the vicinity of the solar system. These include changes in the cosmic ray flux, in the pressure of the different interstellar components and possibly even gravitational tides. On very long time scales, the variations arise from the variable star formation rate of the Milky Way, while on shorter scales, from passages through the galactic spiral arms and vertical oscillations relative to the galactic plane. We also summarize the various records of past variations, in meteorites, in the ocean sea floor and even in various paleoclimatic records.

Keywords: Milky Way, Solar System, Cosmic Ray Flux, Interstellar Medium, Star Formation Rate, Spiral Arms, Meteorites, Climate

1. Introduction

What do we mean by long term variations in the galactic environment? On the time scale of million of years, various parameters characterizing our galactic environment can vary considerably. These include the flux of cosmic rays, the thermal and non-thermal pressure components, the density of interstellar dust and its composition. Even galactic tides which can perturb the Oort cloud can be considered as part of the nearby galactic environment. Some of these factors will be shown to be relatively important.

On various time scales, variations in the galactic environment can arise from different physical processes. For example, very long time scales are governed by variations in the global star formation rate (SFR) of the Milky Way (MW), perhaps affected by nearby passages of the Large Magellanic Cloud (LMC). On somewhat shorter scales, the galactic "ge-

ography" and dynamics, and in particular, its spiral structure becomes important. This is because the environment within spiral arms is notably more "active" than the inter-arm regions. On time scales shorter still, it is the vertical oscillations relative to the galactic plane which become important as do local inhomogeneities in the intergalactic medium. We shall limit ourselves here to time scales longer than about 10^7 years, and therefore will not discuss the "local" inhomogeneities. These will be elaborated in chapter 3.

We begin by reviewing the relevant parameters characterizing the galactic environment and their affect on the solar system. We will then continue with a lengthy description of the different processes governing the *variations* in the galactic environment and the various records we have of them.

2. Characterizing the physical environment

In this section, we briefly review the main environmental parameters influencing the solar system on long time scales. This part is merely intended as a short background. Different processes are elaborated in subsequent chapters. In particular, many of the processes are notably more important on shorter scales, and deserve more elaborate attention.

2.1 Solar wind and interaction with the ISM

The interstellar medium consists of various components each supplying a similar contribution to the total pressure. These include the gas thermal pressure, turbulent pressure, magnetic energy density, as well as cosmic rays and ram pressures from the motion of the solar system. The ram pressure is interesting because it acts very asymmetrically, while the cosmic rays, as we will discuss further below, have additional ways of interacting with the solar system.

The main effect that the ISM pressure has on the solar system is the interaction with the solar wind. At the simplest level, this can be seen as an equilibrium between the solar wind ram pressure $\dot{M}v_{wind}/4\pi R_{helio}^2$ and the total ISM pressure, $P_{\rm ISM}$, which determines the heliopause. The equilibration of the pressures yields a rough estimate of the location of the heliopause:

$$R_{helio} \sim \sqrt{\frac{v_{wind}\dot{M}}{4\pi P_{\rm ISM}}}. \tag{1.1}$$

A higher ISM pressure therefore implies a smaller heliopause, while a higher mass loss rate implies a larger heliopause.

The largest long-term variations in the total ISM pressure arise from the stratified structure, perpendicular to the galactic plane. Various

models yield average profiles for each of the components (e.g., Boulares and Cox, 1990, Ferriere, 1998). The total pressure too decays with height. Over the first 100 pc, it drops by about 20%, or 35% over the first 200 pc. Thus, as the solar system oscillates around the galactic plane (with its current amplitude of about 100 pc, e.g., Bahcall and Bahcall, 1985), this stratification will result with a time variable ISM pressure.

More variations arise from the spiral structure. The spiral density waves are generally $\mathcal{O}(10\%)$ perturbations in the overall density, necessarily giving rise to similar variations in the pressure. However, cold components can be more notably affected by the spiral density wave and even form shocks (e.g., Binney and Tremaine, 1987).

Since typical velocities relative to the ISM are ~ 10 km/s (for example, from the vertical oscillation), the ram pressure can be comparable to the "static" components. It becomes very important if the solar system happens to cross a molecular cloud.

Another interesting effect can take place if the ISM's gas density becomes high enough. The hitherto neglected gravitational field of the sun can become important. As ISM gas approaches the solar system, it accelerates such that an additional ram pressure component is obtained. Once this effect becomes important, the solar wind cannot overcome the infalling ISM material, since both the solar wind and the ISM's accretion ram pressure scale as r^{-2}. Namely, if the effect begins, the solar wind quenches altogether and Bondi accretion of interstellar material takes place unhindered. Talbot and Newman, 1977, estimated that the solar system may have passed 10-100 times during its existence in dense enough clouds for this effect to have taken place. For a 30°K cloud, the critical density is $n_\infty \sim 100$ cm^{-3}.

Under normal conditions, however, when the solar wind is intact, it acts to shield the solar system from low energy cosmic rays and small dust grains.

Interestingly, since the solar rotation is slowly decreasing with time, so is its non-thermal activity and with it so will $\dot{M}$. This is the source of the largest change in the heliopause over time.

By comparing the non-thermal activity (as measured with X-rays), rotation and winds of nearby stars, it is possible to reconstruct the mass loss history of solar-like stars. Wood et al., 2002, find a mass loss which scales as:

$$\dot{M}(t) \propto t^{-2.0\pm0.5}. \tag{1.2}$$

Thus, earlier in the solar system's history, the solar wind was stronger and the heliopause located further out, such that the various effects of the solar wind were more prominent.

2.2 Cosmic Rays

Cosmic Rays are one of the constituents of the interstellar medium, contributing an average pressure comparable to the other ISM components. However, because they "penetrate" the solar wind, they are different from the other components.

In the frame of reference of a random magnetic field, the cosmic rays can be seen to have a random walk. However, since the cosmic rays that managed to reach the inner solar system had net scattering up wind, these cosmic rays lose energy, which is typically ~ 1 GeV.

Their loss of the energy can be parameterized using the modulation parameter Φ. In the limit of high energies ($\gtrsim$1 GeV), the modulation parameter corresponds to the the potential in the force-field approximation (Gleeson and Axford, 1968), given by $\Phi = (R - R_E)v_{wind}/3\kappa_0$ where v_{wind} is the solar wind velocity, κ_0 is the cosmic ray diffusion constant while R is the size of the heliosphere and R_E is the solar-terrestrial distance (= 1 A.U.). Using Φ, we can relate the differential particle density flux near Earth $J(E_k)$ (as a function of the proton kinetic energy E_k) to that outside the solar system $J_0(E_k)$ (e.g., Boella et al., 1998):

$$J(E_k) = J_0(E_k + \Phi)\left[\frac{E_k(E_k + 2m_0c^2)}{(E_k + \Phi)(E_k + \Phi + 2m_0c^2)}\right]. \qquad (1.3)$$

At high energies, the differential particle flux outside the solar system can be approximated with a modified power law $J_0(E_k) = C(E_k + x)^{-2.5}$, where $x = \exp(-2.5 \times 10^{-4} E_k)$ (e.g., Castagnoli and Lal, 1980). Over the solar cycle, the modulation parameter Φ typically varies between 0.2 to 1.2 GeV, with the long-term average being $\Phi = 0.55$ GeV (Ready, 1987).

We can see that varying Φ will have a larger effect on lower energies. Typical energies of interest to us are ~ 1 GeV, which are the energies recorded in spallation products within meteorites or the atmosphere, and ~ 10 GeV which presumably affect climate through modulation of the tropospheric ionization (see §4.3). Thus, if the heliosphere changes by $\mathcal{O}(1)$, as happens regularly over the solar cycle or due to secular changes in solar activity, we expect variations of order $\mathcal{O}(1)$ in the spallation products, while only $\mathcal{O}(10\%)$ for the higher energies that penetrate the troposphere.

Φ also varies through changes in $P_{\rm ISM}$ because of the dependence of Φ on R and R on Φ. The ensuing dependence of the integrated energy flux F reaching Earth, on changes in the ISM pressure, is depicted in fig. 1.1. We see that for high energies, those which are presumably responsible for climate variations, the effect of the varying ISM pressure is relatively

small. On the lower energies which affect the rate of spallation, the variations can be large. Interestingly, flux changes following the reduction in the ISM pressure are more important than increases in $P_{\rm ISM}$. This is because irrespective of the increase in $P_{\rm ISM}$, the ensuing increase in J is capped by J_0. On the other hand, arbitrary reductions in $P_{\rm ISM}$ can arbitrarily increase R and with it decrease J relative to J_0.

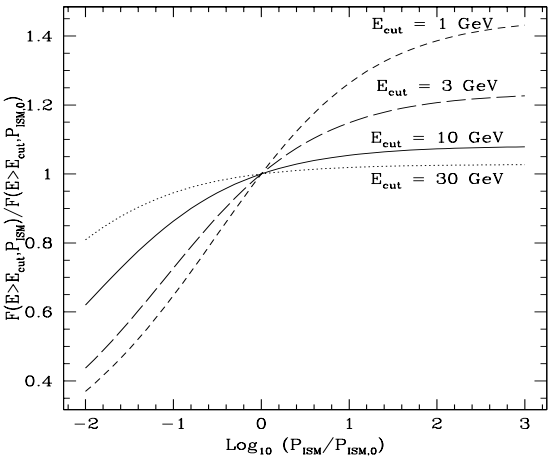

Figure 1.1. The effect that the changed ambient pressure has on the integrated energy flux of cosmic rays reaching Earth, above energies larger than $E_{cut} = 1, 3, 10$ and 30 GeV. At higher energies, the effect is smaller and becomes asymmetric. Moreover, the effect is capped as the pressure is increased—at the value of the flux outside the system.

As an example, changing the pressure by factor of 2 or 0.5 will change the flux by 10% or -10% at an energies of 1 GeV or higher, but only by 2.5% or -3% at energies of 10 GeV. Thus, the vertical oscillations relative to the galactic plane, with an amplitude of ~ 100 pc, or ~ 20% in the pressure, will be a -3% effect at energies larger than 1 GeV or 1% for a 10 GeV cutoff.

In addition to the above variations, which are apparently small and arise from modulations of the heliopause, long time scale variations will also arise from *intrinsic* variations in the cosmic ray flux (CRF) sources. Namely, there will be variations because our solar neighborhood may have more or less supernova taking place in its vicinity. This flux, that reaches the outskirts of solar system is going to be proportional to the rate of nearby supernovae. This, in turn, will depend on various factors. For example, it will depend on the SFR in our galactic neighborhood, on the overall SFR in the Milky Way, or even on local inhomogeneities in the magnetic field which affect the propagation of the cosmic from their sources. This flux will have only a small energy dependence arising from the weak energy dependence of the diffusion parameter describing the diffusion of cosmic rays in the ISM.

3. Variations in the galactic environment

We continue with the study of the physical processes governing the long term variations. These are summarized in fig. 1.2 and include global changes in the SFR (perhaps through gravitational tides induced by LMC perigalactic passages), rotation around the galaxy and the related passages through the galactic spiral arms, as well as vertical oscillations relative to the plane of the Milky Way.

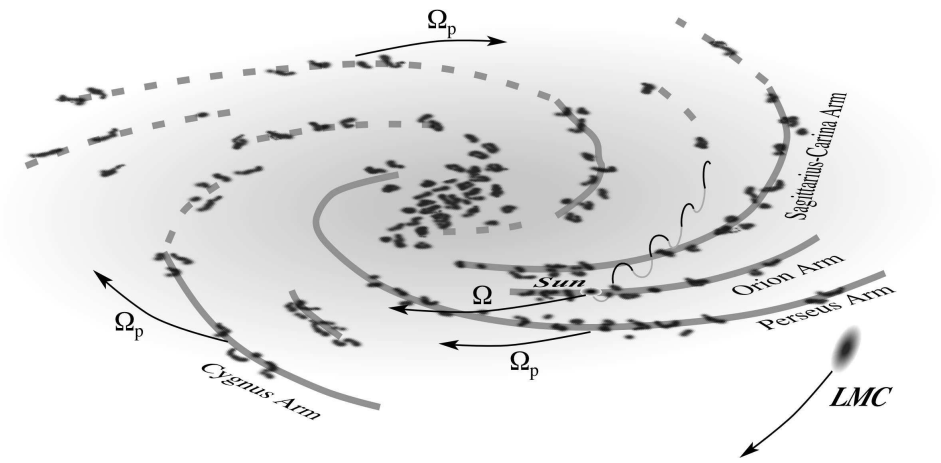

Figure 1.2. A simplified heuristic cartoon of the Milky Way and the causes for long term variations in the galactic environment. On the longest time scales (few 10^9 yr or longer), there are global variations in the MW's SFR (any variations measured using nearby stars is necessarily global through azimuthal diffusion). These may be influenced from nearby passages of the LMC—the last two perigalactic passages do appear to coincide with increased SFR in both the MW and the LMC. On time scales of 10^8 yr, we have passages through the galactic spiral arms. The actual spiral structure is probably more complicated than illustrated. In particular, it is hard to reconstruct the spiral structure within the solar circle because of the azimuthal ambiguity of velocity-longitude maps, which yield a clear structure only outside the solar circle (e.g., Blitz et al., 1983, Dame et al., 2001). Thus, spiral arms marked with a "dashed line" should be considered cautiously. Secondly, there is mounting evidence that the spiral arms observed are actually part of at least two sets (which happen to roughly coincide today), each having a different pattern speed (Shaviv, 2003a, Naoz and Shaviv, 2004). Compounded on that, we are currently located on the Orion "spur", moving at roughly the same speed as the solar system (Naoz and Shaviv, 2004). We may have passed through other such spurs in the past. On the shortest time scale, the solar system performs vertical oscillations, such that every few 10^7 yr, it crosses the galactic plane.

3.1 Star Formation Rate

The local and overall SFR in the MW are not constant. These variations will in turn control the rate of supernovae. Moreover, supernova

remnants accelerate cosmic rays (at least with energies $\lesssim 10^{15}$ eV), and inject fresh high-Z material into the galaxy. Thus, cosmic rays and galactic nuclear enrichment, is proportional to the SFR.

Although there is a lag of several million years between the birth and death of massive stars, this lag is small when compared to the relevant time scales at question. Over the 'short term', i.e., on time scales of 10^8 yr or less, the record of nearby star formation is 'Lagrangian', i.e., the star formation in the vicinity of the moving solar system. This should record passages through galactic spiral arms. On longer time scales, of order 10^9 yr or longer, mixing is efficient enough to homogenize the azimuthal distribution in the Galaxy (Wielen, 1977). In other words, the long-term star formation rate, as portrayed by nearby stars, should record the long term changes in the Milky Way SFR activity. These variations may arise, for example, from a merger with a satellite or a nearby passage of one.

Scalo, 1987, using the mass distribution of nearby stars, concluded that the SFR had peaks at 0.3 Gyr and 2 Gyr before present (b.p.). Barry, 1988, and a more elaborate and recent analysis by Rocha-Pinto et al., 2000, measured the star formation activity of the Milky Way using chromospheric ages of late type dwarfs. They found a dip between 1 and 2 Gyr and a maximum at 2-2.5 Gyr b.p.[1] (see also fig. 1.3).

Another approach for the reconstruction of the SFR, is to use the cluster age distribution. A rudimentary analysis reveals peaks of activity around 0.3 and 0.7 Gyr b.p., and possibly a dip between 1 and 2 Gyr (as seen in fig. 1.3). A more recent analysis considered better cluster data and only nearby clusters, closer than 1.5 kpc (de La Fuente Marcos and de La Fuente Marcos, 2004). Besides the above peaks which were confirmed with better statistical significance, two more peaks were found at 0.15 and 0.45 Gyr. At this temporal and spatial resolution, we are seeing the spiral arm passages. On longer time scales, cluster data reveals a notable dip between 1 and 2 Gyr (de La Fuente Marcos and de La Fuente Marcos, 2004, Shaviv, 2003a).

3.2 Spiral Arm passages

On time scales shorter than those affecting global star formation in the Milky Way, the largest perturber of the local environment is our passages through the galactic spiral arms.

[1]There are contradicting results by Hernandez et al., 2000, but this analysis assumes that the stars in the solar vicinity has the same metalicity as the sun, and it also assumes implicitly that the SFR today necessarily approaches zero. Thus, this discrepancy is not a source of concern.

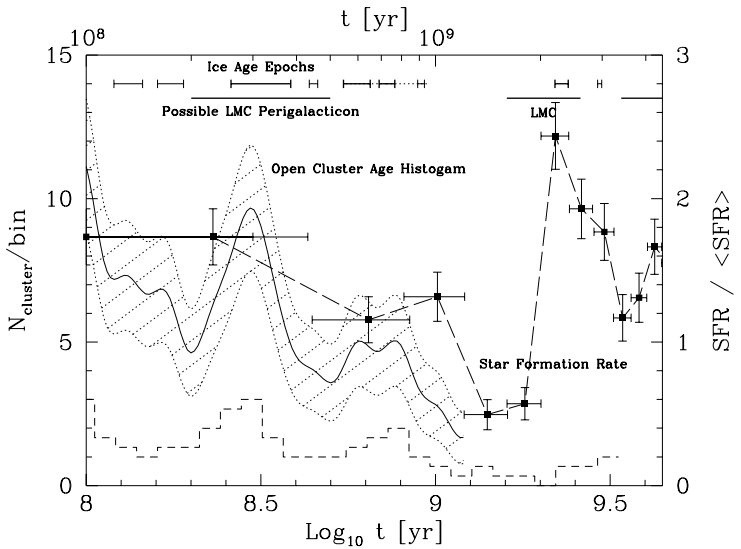

Figure 1.3. The history of the SFR. The squares with error bars are the SFR calculated using chromospheric ages of nearby stars (Rocha-Pinto et al., 2000). These data are corrected for different selection biases and are binned into 0.4 Gyr bins. The line and hatched region describe a 1-2-1 average of the histogram of the ages of nearby open clusters using the Loktin et al., 1994, catalog, and the expected 1-σ error bars. These data are not corrected for selection effects (namely, the upward trend with time is a selection effect, favorably selecting younger clusters more of which did not yet dissolve). Since the clusters in the catalog used are spread to cover two nearby spiral arms, the signal arising from the passage of spiral arms is smeared, such that the graph depicts a more global SFR activity (i.e., in our galactic 'quadrant'). On longer time scales (1.5 Gyr and more), the galactic azimuthal stirring is efficient enough for the data to reflect the SFR in the whole disk. There is a clear minimum in the SFR between 1 and 2 Gyr BP, and there are two prominent peaks around 0.3 and 2.2 Gyr BP. Interestingly, the LMC perigalacticon should have occurred sometime between 0.2 and 0.5 Gyr BP in the last passage, and between 1.6 and 2.6 Gyr BP in the previous passage. This might explain the peaks in activity seen. This is corroborated with evidence of a very high SFR in the LMC about 2 Gyr BP and a dip at 0.7-2 Gyr BP (Gardiner et al., 1994, Lin et al., 1995). Also depicted are the periods during which glaciations were seen on Earth: The late Archean (3 Gyr) and mid-Proterozoic (2.2-2.4 Gyr BP) which correlate with the previous LMC perigalacticon passage (Gardiner et al., 1994, Lin et al., 1995) and the consequent SFR peak in the MW and LMC. The lack of glaciations in the interval 1-2 Gyr b.p. correlates with a clear minimum in activity in the MW (and LMC). Also, the particularly long Carboniferous-Permian glaciation, correlates with with the SFR peak at 300 Myr BP and the last LMC perigalacticon. The late Neo-Proterozoic ice ages correlate with a less clear SFR peak around 500-900 Myr BP.

The period with which spiral arms are traversed depends on the relative angular speed around the galaxy, between the solar system with

$\Omega_\odot$ and the spiral arms with Ω_p:

$$\Delta T = \frac{2\pi}{m\,|\Omega_\odot - \Omega_p|}, \tag{1.4}$$

where m is the number of spiral arms.

Our edge-on vantage point is unfortunate in this respect, since it complicates the determination of both the geometry and the dynamics of the spiral arms. This is of course required for the prediction of the spiral arm passages. In fact, the understanding of neither has reached a consensus.

Claims in the literature for a 2-armed and a 4-armed structure are abundant. There is even a claim for a combined 2+4 armed structure (Amaral and Lepine, 1997). Nevertheless, if one examines the $v-l$ maps of molecular gas, then it is hard to avoid the conclusion that *outside* the solar circle, there are 4 arms[2]. Within the solar circle, however, things are far from clear. This is because $v-l$ maps become ambiguous for radii smaller than $R_\odot$, such that each arm is folded and appears twice. Shaviv, 2003a, has shown that if the outer 4-arms obey the simple density wave dispersion relation, such that they cannot exist beyond the 4:1 Lindblad resonances then two sets of arms should necessarily exist. In particular, the fact that these arms are apparent out to $r_{out} \approx 2R_\odot$ necessarily implies that their inner extent, the inner Lindblad radius, should roughly be at $R_\odot$. Thus, the set of arms internal to our radius should belong to a set other than the outer 4 arms.

The dynamics, i.e., the pattern speed of the arms, is even less understood that the geometry. A survey of the literature (Shaviv, 2003a) reveals that about half of the observational determinations of the relative pattern speed $\Omega_\odot - \Omega_p$ cluster around $\Omega_\odot - \Omega_p \approx 9$ to 13 km s^{-1}kpc^{-1}, while the other half are spread between $\Omega_\odot - \Omega_p \approx -4$ and 5 km s^{-1}kpc^{-1}. In fact, one analysis (Palous et al., 1977) revealed that both $\Omega_\odot - \Omega_p =$ 5 and 11.5 km s^{-1}kpc^{-1} fit the data equally well.

Interestingly, if spiral arms are a density wave (Lin and Shu, 1964), as is commonly believed (e.g., Binney and Tremaine, 1987), then the observations of the 4-armed spiral structure in HI outside the Galactic solar orbit (Blitz et al., 1983) severely constrain the pattern speed to satisfy $\Omega_\odot - \Omega_p \gtrsim 9.1 \pm 2.4$ km s^{-1}kpc^{-1}, since otherwise the four armed density wave would extend beyond the outer 4 to 1 Lindblad resonance (Shaviv, 2003a).

This conclusion provides theoretical justification for the smaller pattern speed. However, it does not explain why numerous different es-

[2]Actually, 3 are seen, but if a roughly symmetric set is assumed, then a forth arm should simply be located behind the galactic center.

timates for Ω_p exist. A resolution of this "mess" arises if we consider the possibility that at least two spiral sets exist, each one having a different pattern speed. Indeed, in a stellar cluster birth place analysis, which allows for this possibility, it was found that the Sagittarius-Carina arm appears to be a superposition of two arms (Naoz and Shaviv, 2004). One has a relative pattern speed of $\Omega_\odot - \Omega_{P,Carina,1} = 10.6^{+0.7}_{-0.5sys} \pm 1.6_{stat}$ km s^{-1}kpc^{-1} and appears also in the Perseus arm external to the solar orbit. The second set is nearly co-rotating with the solar system, with $\Omega_\odot - \Omega_{P,Carina,2} = -2.7^{+0.4}_{-0.5sys} \pm 1.3_{stat}$ km s^{-1}kpc^{-1}. The Perseus arm may too be harboring a second set. The Orion "armlet" where the solar system now resides (and which is located in between the Perseus and Sagittarius-Carina arms), appears too to be nearly co-rotating with us, with $\Omega_\odot - \Omega_{p,Orion} = -1.8^{+0.2}_{-0.3sys} \pm 0.7_{stat}$ km s^{-1}kpc^{-1}.

For comparison, a combined average of the 7 previous measurements of the 9 to 13 km s^{-1}kpc^{-1} range, which appears to be an established fact for both the Perseus and Sagittarius-Carina arms, gives $\Omega_\odot - \Omega_p = 11.1 \pm 1$ km s^{-1}kpc^{-1}. At reasonable certainly, however, a second set nearly co-rotating with the solar system exists as well.

The relative velocity between the solar system and the first set of spiral arms implies that every ~ 150 Myr, the environment near the solar system will be that of a spiral arm. Namely, we will witness more frequent nearby supernovae, more cosmic rays, more molecular gas as well as other activity related to massive stars. We will show below that there is a clear independent record of the passages through the arms of the first set. On the other hand, passages through arms of the second set happen infrequently enough for them to have been reliably recorded.

3.3 Vertical motion in the galactic disk

In addition to the revolutions around the galaxy, the solar system also performs vertical oscillations relative to the disk. Since the potential is not Keplerian, the period of the vertical oscillations is different from the orbital period. Because mass is concentrated towards the galactic plane, the vertical motions depend primarily on the amount of mass in the disk. If one assumes a constant mass density ρ_m, then the frequency will be given by:

$$\Omega_v = \sqrt{4\pi G \rho_m}. \tag{1.5}$$

More than two dozen estimates for ρ_m range from between 0.05 to 0.25 $M_\odot\ pc^{-3}$, such that Ω_v is not known accurately enough. Although it is not clear that averaging of the different results obtained in various methods is legitimate, it yields a half period (i.e., plane crossing inter-

vals) of $P_v/2 = 35 \pm 8$ Myr (Matese et al., 1995), or even 37 ± 4 Myr (Stothers, 1998).

Estimates for the phase of this oscillation are better constrained. This is because we are near the galactic plane, having recently crossed it and now moving upwards, away from it. This implies that we last crossed the plane roughly before $T_{cross} \approx 0 - 5$ Myr, based on the estimates of 1.5 ± 1.5 Myr (Bahcall and Bahcall, 1985, 5 ± 5 Myr (Rampino and Stothers, 1986) and 4 ± 2 Myr (Shoemaker and Wolfe, 1986).

At this periodicity, we should witnessed several effects. First, the stratified structure implies that the pressure closer to the center of the plane is higher. For the current amplitude, which is ~ 100 pc, the pressure variations are $\sim 20\%$. This implies a heliopause which is typically 10% smaller.

Second, the vertical oscillations will also imply variations in the CRF. The smaller source of variations originates from the varying size of the heliopause, thereby modulating the CRF. However, this effect is going to be of order $\sim 3\%$ at the low energies which affect spallation, and negligible at the higher energies affecting tropospheric ionization. The larger variations in the CRF will come from the vertical stratification in the CRF distribution. Typical estimates for the CRF density give a 10% decrease over the 100 pc amplitude of the vertical oscillations (e.g., Boulares and Cox, 1990).

Third, passages through the galactic plane impose galactic tides which can perturb the Oort cloud. This, in turn, can send a larger flux of comets into the inner solar system (Torbett, 1986, Heisler and Tremaine, 1989), which can either hit directly (and leave a record as craters or cause mass extinction, Rampino and Stothers, 1984), or affect climate through disintegration in the atmosphere (Napier and Clube, 1979, Alvarez et al., 1980) or disintegrate and be accreted as dust (Hoyle and Wickramasinghe, 1978).

4. Records of long term variations

In this section, we will concentrate on the various records registering the long period variations in the solar system's environment. These include different records of the CRF, and of accreted interstellar material.

4.1 Cosmic ray record in Iron meteorites

Various small objects in the solar system, such as asteroids or cometary nuclei, break apart over time. Once the newly formed surfaces of the debris are exposed to cosmic rays, they begin to accumulate spallation products. Some of the products are stable and simply accumulate with

time, while other products are radioactive and reach an equilibrium between the formation rate and their radioactive decay. Some of this debris reaches Earth as meteorites. Since Chondrites (i.e., stony) meteorites generally "crumble" over $\lesssim 10^8$ yr, we have to resort to the rarer Iron meteorites, which crumble over $\lesssim 10^9$ yr, if we wish to study the CRF exposure over longer time scales.

The cosmic ray exposure age is obtained using the ratio between the amount of the accumulating and the unstable nuclei. Basically, the exposure age is a measure of the integrated CRF, as obtained by the accumulating isotope, in units of the CRF "measured" using the unstable nucleus. Thus, the "normalization" flux depends on the average flux over the last decay time of the unstable isotope and not on the average flux over the whole exposure time. If the CRF is assumed constant, then the flux obtained using the radioactive isotope can be assumed to be the average flux over the life of the exposed surface. Only in such a case, can the integrated CRF be translated into a real age.

Already quite some time ago, various groups obtained that the exposure ages of Iron meteorites based on "short" lived isotopes (e.g., ^{10}Be) are inconsistent with ages obtained using the long lived unstable isotope ^{40}K, with a half life of ~ 1 Gyr. In essence, the first set of methods normalize the exposure age to the flux over a few million years or less, while in the last method, the exposure age is normalized to the average flux over the life time of the meteorites. The inconsistency could be resolved only if one concludes that over the past few Myr, the CRF has been higher by about 30% than the long term average (Hampel and Schaeffer, 1979, Schaeffer et al., 1981, Aylmer et al., 1988, Lavielle et al., 1999).

More information on the CRF can be obtained if one make further assumptions. Particularly, if one assumes that the parent bodies of Iron meteorites tend to break apart at a constant rate (or at least at a rate which only has slow variations), then one can statistically derive the CRF history. This was done by Shaviv, 2003a, using the entire set of ^{40}K dated Iron meteorites. To reduce the probability that the breaking apart is real, i.e., that a single collision event resulted with a parent body braking apart into many meteorites, each two meteorites with a small exposure age difference (with $\Delta a \leq 5 \times 10^7$ yr), and with the same Iron group classification, were replaced by a single effective meteor with the average exposure age.

If the CRF is variable, then the exposure age of meteorites will be distorted. Long periods during which the CRF was low, such that the exposure clock 'ticked' slowly, will appear to contract into a short period in the exposure age time scale. This implies that the exposure ages of

meteorites is expected to cluster around (exposure age) epochs during which the CRF was low, while there will be very few meteors in periods during which the CRF was high.

Over the past 1 Gyr recorded in Iron meteorites, the largest variations are expected to arise from our passages through the galactic spiral arms. Thus, we expect to see cluster of ages every $\sim$ 150 Myr. The actual exposure ages of meteorites are plotted in fig. 1.4, where periodic clustering in the ages can be seen. This clustering is in agreement with the expected variations in the cosmic ray flux. Namely, Iron meteorites recorded our passages through the galactic spiral arms.

Interestingly, this record of past cosmic ray flux variations and the determination of the galactic spiral arm pattern speed is different in its nature from the astronomical determinations of the pattern speed. This is because the astronomical determinations assume that the sun remained in the same galactic orbit it currently occupies. The meteoritic measurement is "Lagrangian". It is the measurement relative to a moving particle, our solar system, which could have had small variations in its orbital parameters. In fact, because of the larger solar metalicity than the solar environment, the solar system is more likely to have migrated outwards than inwards. This radial diffusion gives an error and a bias when comparing the effective, i.e., "Lagrangian" measured $\tilde{\Omega}_p$, to the "Eularian" measurements of the pattern speed:

$$\tilde{\Omega}_p - \Omega_p = 0.5 \pm 1.5 \text{ km s}^{-1}\text{kpc}^{-1} \tag{1.6}$$

Taking this into consideration, the observed meteoritic periodicity, with $P = 147 \pm 6$ Myr, implies that $\Omega_\odot - \Omega_p = 10.2 \pm 1.5_{sys} \pm 0.5_{stat}$, where the systematic error arises from possible diffusion of the solar orbital parameters. This result is consistent with the astronomically measured pattern speed of the first set of spiral arms.

4.2 Accretion of extraterrestrial dust

One of the interesting effects of the solar wind is the shielding against the penetration of small ISM grains. Namely, grains smaller than about 10^{-13} gr are blocked from entering the solar system through electromagnetic interaction with the solar wind's magnetic field. The flux of the more massive dust particles which can penetrate the solar system, and be accreted on Earth, is typically $\sim$ 1 ton/yr globally (Frisch, 1999, Landgraf et al., 2000). However this should vary depending on the state of the heliosphere.

The interstellar origin of the dust can be identified through its kinematics (high velocity and retrograde orbits). For comparison, the flux of accreted interplanetary dust, is much higher at $\sim$ 100 kton/yr (Kyte and

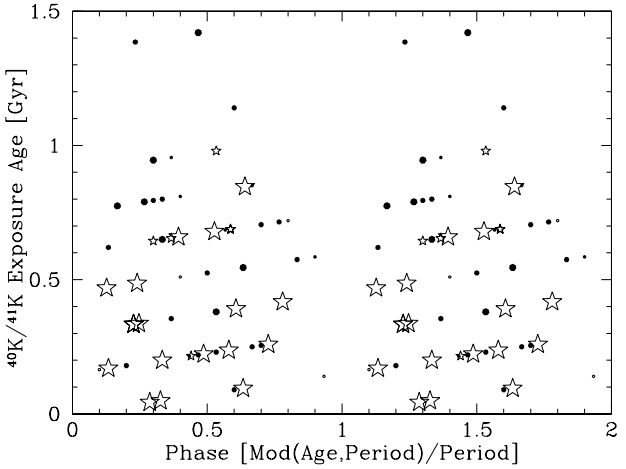

Figure 1.4. The exposure age of Iron meteorites plotted as a function of their phase in a 147 Myr period. The dots are the ^{40}K exposure ages (larger dots have lower uncertainties), while the stars are ^{36}Cl based measurements. The K measurements do not suffer from the long term "distortion" arising from the difference between the short term (10 Ma) CRF average and the long term (1 Gyr) half life of K (Lavielle et al. 1999). However, they are intrinsically less accurate. To use the Cl data, we need to "correct" the exposure ages to take into account this difference. We do so using the result of Lavielle et al. (1999). Since the Cl data is more accurate, we use the Cl measurement when both K and Cl are available for a given meteorite. When less than 50 Ma separates several meteorites of the same Iron group classification, we replace them with their average in order to discount for the possibility that one single parent body split into many meteorites. We plot two periods such that the overall periodicity will be even more pronounced. We see that meteorites avoid having exposure ages with given phases (corresponding to epochs with a high CRF). Using the Rayleigh Analysis, the probability of obtaining a signal with such a large statistical significance as a fluke from random Poisson events, with *any* period between 50 and 500 Ma, is less than 0.5%. The actual periodicity found is 147 ± 6 Myr, consistent with both the astronomical and geological data.

Wasson, 1986). The latter is also comparable to the long term average injection of volcanic ash into the stratosphere.

Because of the small fraction of ISM dust from the total accretion, such material can be detected only by identifying extra-solar fingerprints. Such a record exists in the form of non-cosmogenically produced radioactive isotopes. For example, ^{244}Pu has a half live $\sim 10^8$ yr, any natural occurrence must originate from extraterrestrial dust coming from a nearby SN. However, nominal estimates for its flux are at 10 times larger than the actual measurement from scraped deposition on the ocean floor. Only an upper limit could be placed, because the detected amount of ^{244}Pu is consistent with the fallout from manmade nuclear experiments

(Paul, 2001). This is yet an unresolved problem. Current undergoing measurement of ^{244}Pu in ocean floor cores would help us understand the history of the interstellar dust around us, and its relation to SN.

As for the much larger amounts of accreted interplanetary material, the historic flux of fine planetary dust can be reconstructed using the concentration of ^{3}He extracted from ocean floor cores (Farley, 1995). This is possible once the sedimentation rate is accounted for. This reconstruction, over the past 70 Myr is plotted in fig. 1.9.

From the figure, it is evident that the extraterrestrial dust flux is not constant. In fact, notably higher accretion rates took place recently, (in the past few Myr), at $\sim$ 35 Myr and $\sim$ 70 Myr. This is consistent in phase and period with our passages through the galactic plane, though unfortunately not yet statistically significant.

One plausible explanation is that comets are more often injected from the Oort cloud into the inner solar system, due to the gravitational perturbations. The first suggestion was of perturbations from a gravitational impulse of nearby passage of a molecular cloud (Rampino and Stothers, 1984). Perturbations by the potential of the galactic disk were later found to be more important (Heisler and Tremaine, 1986, Torbett, 1986, Heisler et al., 1987, Matese and Whitman, 1989).

Nevertheless, because the link with plane crossing is not firm, other possibilities should be considered too. For example, the Oort cloud could be periodically perturbed by a companion ("Nemesis") each time it reaches perihelion (Davis et al., 1984). In this case, the coincidence with the phase and period of the galactic plane passages should be considered a coincidence.

4.3 Climate Record and the Cosmic Ray Flux

Recent empirical evidence suggests that the cosmic ray flux may be affecting the terrestrial climate. If so, it would imply that any long term climate record could be registering the "historic" CRF variations, and with it, the environment of the solar system. We begin with a short summary of this empirical evidence (see Chapter 10 for a lengthy review of the topic), and continue with the geological record of long term climate variations.

Accumulating evidence suggests that solar activity is responsible for at least some climatic variability. These include correlations between solar activity and either direct climatic variables or indirect climate proxies over time scales ranging from days to millennia (e.g., Herschel, 1796, Eddy, 1976, Labitzke and van Loon, 1992, Lassen and Friis-Christensen, 1995, Svensmark and Friis-Christensen, 1997, Soon et al., 1996, Soon

et al., 2000, Beer et al., 2000, Hodell et al., 2001, Neff et al., 2001). It is therefore difficult at this point to argue against the existence of any causal link between solar activity and climate on Earth. However, the climatic variability attributable to solar activity is larger than could be expected from the typical 0.1% changes in the solar irradiance observed over the decadal to centennial time scale (Beer et al., 2000, Soon et al., 2000). Thus, an amplifier is required unless the sensitivity to changes in the radiative forcing is uncomfortably high.

The first suggestion for an amplifier of solar activity was suggested by Ney, 1959, who pointed out that if climate is sensitive to the amount of tropospheric ionization, it would also be sensitive to solar activity since the solar wind modulates the CRF, and with it, the amount of tropospheric ionization. An indeed, over the solar cycle, the solar wind strength varies considerably, such that the amount of tropospheric ionization changes by typically 5%-10% (see §2). Moreover, several recent analysis (Svensmark, 1998, Svensmark, 2000, Marsh and Svensmark, 2000, as well as Palle Bago and Butler, 2000) have shown that the variations in the amount of low altitude cloud cover (LACC) nicely correlate with the CRF reaching Earth over two decades of solar variations.

One of the points raised as a critique of the CRF→LACC link is that the empirical correlation between CRF variations and the LACC arise when comparing any solar activity index, such that a mere correlation is not sufficient to prove the link. However, as we shall see below, also intrinsic variations in the CRF correlate with climate. Moreover, a recent analysis (Usoskin et al., 2004) reveals that geographically, the CRF/LACC correlation is as predicted. Namely, the amount of cloud cover change over the solar cycle at different latitudes is proportional to the change in tropospheric ionization averaged over the particular latitudes. Secondly, there is growing theoretical and empirical evidence linking tropospheric ionization to the formation of condensation nuclei. In particular, Yu, 2002, has shown how modification of the ionization rate could affect the formation of condensation nuclei (CN) primarily at low altitudes, where ions are scarce. Eichkorn et al., 2002, have shown using airborne observations that the formation of CN is indeed linked to charge, while Harrison and Aplin, 2001, have shown that the formation of CN correlates with natural Poisson variability in the CRF. It has yet to be proved that the formation of CN does affect cloud condensation nuclei (CCN). Namely, that CN grow by mutual coalescence as opposed to being scavenged by the already large CCN.

Chapter 10 includes a more elaborate discussion of the possible cosmic ray flux link. Here we shall explore the ramifications of this link on long, i.e., geological time scales.

4.3.1 Earths glacial activity and the Star Formation Rate.

On the longest time scales, i.e., over Earth's entire history, the largest variations in the cosmic ray flux arise from of the Milky Way's star formation activity. Over these time scales, however, there are other large sources of climate variations which we should consider if we are to look for the signature of the SFR variability.

According to standard solar models, the solar luminosity increased from about 70% of the present solar luminosity at 4.5 Gyr b.p., to its present value. If Earth were a black body, its temperature would have been 25°K lower, enough to have kept large parts of it frozen until about 1-2 Gyr b.p. Besides however the past Eon, and the Eon between 2 and 3 Gyr b.p., it appears that glaciations were altogether absent from the global surface. This is the crux of the so called faint Sun paradox (Sagan and Mullen, 1972, Pollack, 1991, Sagan and Chyba, 1997).

Various types of solutions exist. Some utilize various greenhouse gases. In particular, it was suggested that small amounts of NH_3 could have supplied the required GHG warming (Sagan and Mullen, 1972, Sagan and Chyba, 1997). Although not impossible, it is not easy to keep NH_3 from irreversibly photolyzing into H_2 and N_2. Another suggestion was that CH_4 played the major GHG warmer (Pavlov et al., 2000). This solution requires a long residency time of methane in the atmosphere, and probably dominance of methanogenic bacteria.

Interestingly, CO_2 was also suggested as a possible greenhouse solution (Kuhn and Kasting, 1983, Kasting, 1993). However, it probably cannot resolve by itself the faint sun paradox because the amounts required to keep Earth warm enough are huge (several bars), and more than some geological limits (e.g., Rye et al., 1995 find $pCO_2 \leq 10^{-1.4}$ bar between 2.2 and 2.7 Gyr before present).

If cosmic rays do affect climate, then the faint sun paradox can be notably extenuated, through the following scenario:

Younger sun rotated faster and was more active
↓
The solar wind was stronger and heliopause further out
↓
CRF reaching earth was lower, as was the tropospheric ionization
↓
CRF/climate effect contributed a warming, compensating the faint sun.

For nominal numbers obtained over the Phanerozoic (past 550 Million years), this effect translates to a compensation of half to two thirds of the faint sun paradox (Shaviv, 2003b).

On top of the above processes, we are now in a position to consider the effect of a variable SFR. This is done by assuming that the CRF reaching

the outskirts of the solar system is not constant, but proportional to the Milky Way's SFR. This is done in fig. 1.5 while considering the SRF obtained by Rocha-Pinto et al., 2000.

The figure demonstrates that, (a) the weakening solar wind and ensuing increased CRF can compensate for about half of the faint sun paradox. Together with moderate greenhouse warming (e.g., with reasonably higher levels of CO_2) the faint sun paradox can be resolved. (b) The varying star formation introduces a large effect. It explains why the temperature was on average colder over the last Eon and between 2 and 3 Gyr ago, enough to explain the appearance of ice-epochs, while the lower SFR between 1 and 2 Gyr before present explains the increased temperature and total lack of glacial activity. And (c) the compensation that the reduced solar wind/increased CRF has on the increasing solar luminosity is reaching its end, since almost all the CRF at ~ 10 GeV is reaching Earth. The temperature will therefore increase in the future, albeit on very long time scales!

4.3.2 Ice-Age Epochs and Spiral arm passages. If the proposed CRF/climate link is real, then the periodic CRF variations arising from our passages through the galactic spiral arms, and measured in Iron meteorites, necessarily imply that cold epochs should arrive every ~ 145 Myr on average.

Under typical diffusion parameters, the cosmic ray density contrast between spiral arms and the inter-arm region is expected to be between about 2 to 6 (Shaviv, 2003a). This is consistent with the meteoritic exposure age data, which gives a contrast larger than 2.5 (Shaviv, 2003a). An upper limit cannot be placed because of the statistical error in the exposure ages of the meteorites.

The large $\mathcal{O}(1)$ variations in flux imply large variations in temperature, of order $\sim 5°$K globally. Thus, each spiral arm crossing the average temperature is expected to decrease sufficiently to either hinder or trigger the appearance of ice-age epochs (IAE) on Earth.

The correlations between the different celestial and terrestrial records is seen in figs. 1.6-1.8. The statistical significance of the correlations is difficult to asses. This is because various assumptions on the assumed priors necessarily affect the implied significance.

For example, if one *just* compares the occurrence of ice-age epochs as obtained using the sedimentation record, with the CRF signal reconstructed using the meteoritic data, then a minimum χ^2/ν of about 0.5 is obtained (with $\nu = 6$ being the effective number of degrees of freedom). The ice-age epochs lag behind the spiral arm passage by 33 ± 20 Myr, while the prediction is a lag of 28 ± 7 Myr, arising from the skewness of

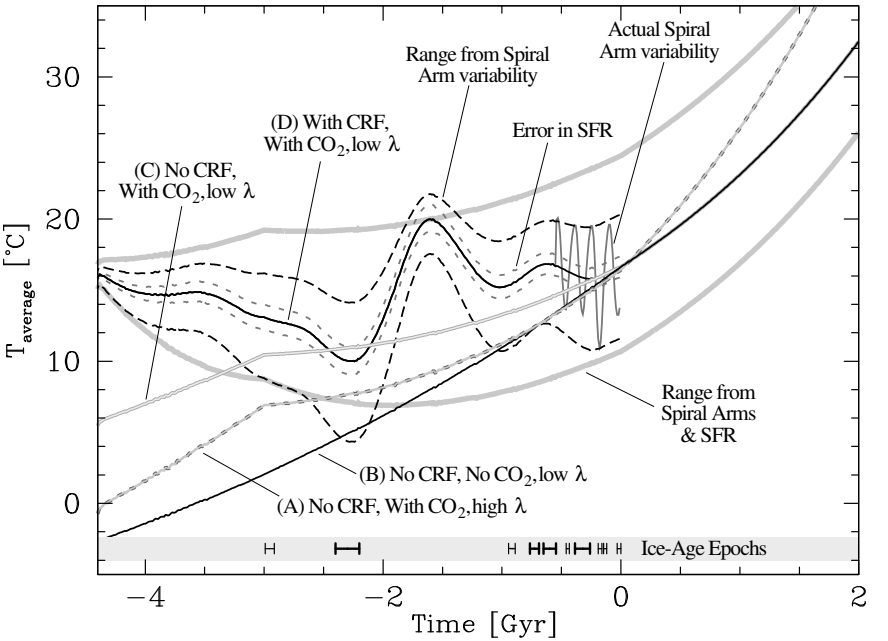

Figure 1.5. Predicted temperature as a function of time before present for various models (as elaborated in Shaviv, 2003b) but using more recent data on climate sensitivity). Model A includes a nominal global temperature sensitivity of $\lambda = 0.54°C/(W/m^2)$ obtained from various paleoclimatic data (Shaviv, 2004) while neglecting a CRF / climate link (λ is the change in the average global temperature associated with a change of 1 W/m^2 in the radiative budget). The model also assumed GHG warming by modest levels of CO_2, not larger than the geological constraints (0.01 bar of CO_2 before 3 Gyr and exponentially decreasing afterward to current levels). Model B includes no CO_2 contribution, but a lower sensitivity of $\lambda = 0.35°C/(W/m^2)$ (close to that of a black body Earth). It is the nominal sensitivity obtained from paleoclimate data while assuming the CRF/climate link is valid (Shaviv, 2004). Model C has both CO_2 and the sensitivity of model B, but still has no CRF contribution. Model D includes a CRF contribution using nominal values for its effect ($\mu \equiv -\Phi_0(dT_{global}/d\Phi_{CR}) = 6.5°$K, Shaviv, 2004). The additional lines give the variations expected or observed from spiral arm passages and SFR variations. Since these cannot be predicted, we only plot the total expected range of variations in the future. Since almost all the 10 GeV CRF (causing tropospheric ionization) currently reaches the inner solar system, this compensation cannot continue, and the temperature will start to significantly increase in the future.

the CRF distribution towards the trailing side of the arm and the lag between an arm passage and the average SN event (Shaviv, 2003a).

To estimate the significance of this correlation, one can try and calculate the probability that a random distribution of IAEs could generate a χ^2 result which is as small as previously obtained. To do so, glaciation epochs where randomly realized and compared with the occurrence of IAEs (Shaviv, 2002). To mimic the effect that nearby glaciations

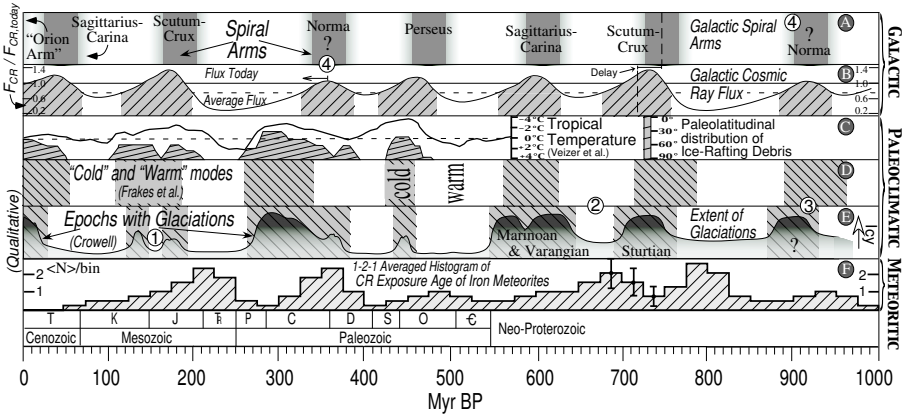

Figure 1.6. Earth's recent history. The top panel (A) describes passages through the Galactic arms assuming a relative pattern speed of $\Omega_p - \Omega_\odot = -11.0$ km s^{-1}kpc^{-1}, which best fits the ice-age epochs (IAEs). Panel (B) describes the Galactic CRF reaching the solar system using a CR diffusion model, in units of the current day CRF. An important feature is that the flux distribution around each spiral arm is lagging behind spiral arm crossings. This can be seen with the hatched regions in the second panel, which qualitatively show when IAEs are predicted to occur if the critical CRF needed to trigger them is the average CRF. Two dashed lines mark the middle of the spiral crossing and to the expected mid-glaciation point. Panels (C) (D) and (E) describe the paleoclimatological record of the past Eon. The solid line in panel (C) depicts the tropical sea surface temperatures relative to today, as inferred from calcite and aragonite shells in the past ~ 550 Myr. The filled areas describe the paleolatitudinal distribution of ice rafted debris (both from Veizer et al., 2000). Panel (D) and (E) qualitatively describes the epochs during which Earth experienced ice-ages, the top part as described by Frakes et al., 1992, while the bottom one by Crowell, 1999. The Phanerozoic part of panel E is directly taken from Crowell, 1999. Note that (1) The mid-Mesozoic ice-ages did not have true polar caps but were certainly colder than average. (2) Around 650 Myr, Earth still was relatively cold, but still warmer than nearby epochs. (3) The existence of an IAE at 900 Myr is inconclusive. (4) The Norma arm's location is actually a logarithmic spiral extrapolation from its observations at somewhat smaller Galactic radii (Leitch and Vasisht, 1998, Taylor and Cordes, 1993). However, since it is now clear that the inner set probably has nothing to do with the outer spiral set, a more probable location for the "outer" Norma arm, would be symmetrically between its neighboring arms. Note also that the correlations do not have to be absolute since additional factors may affect the climate (e.g., continental structure, atmospheric composition, etc.). Panel (F) is a 1-2-1 smoothed histogram of the exposure ages of Fe/Ni meteors. The meteor exposure ages are predicted to cluster around epochs with a lower CRF flux.

might appear as one epoch, glaciations that are separated by less than 60 Myr were bunched together (which is roughly the smallest separation between observed glaciations epochs). The fraction of random configurations that surpassed the χ^2 obtained for the best fit found using the real data is of order 0.1% for *any* pattern speed. (If glaciations are not

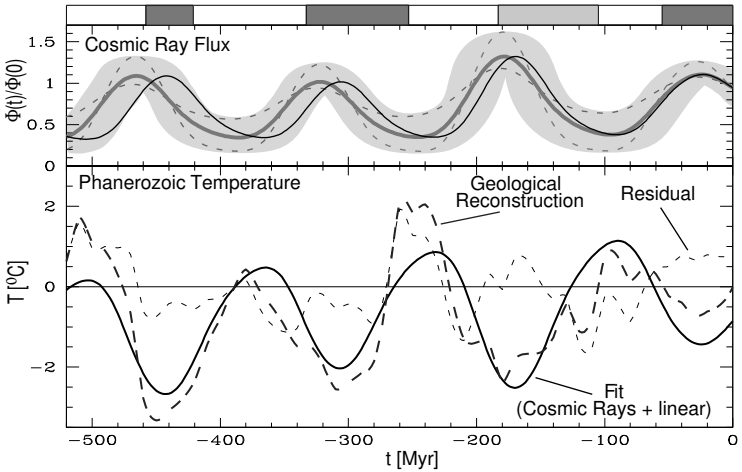

Figure 1.7. The cosmic ray flux (Φ) and tropical temperature anomaly (ΔT) variations over the Phanerozoic (Shaviv and Veizer, 2003). The upper curves describe the reconstructed CRF using iron meteorite exposure age data (Shaviv, 2003a). The heavy gray line depicts the nominal CRF, while the shading delineates the allowed error range. The two dashed curves are additional CRF reconstructions that fit within the acceptable range. The solid black curve describes the nominal CRF reconstruction after its period was fine tuned, within the measurement error, to best fit the low-latitude temperature anomaly. The bottom dashed curve depicts the temperature reconstruction, measured with a 10 Myr bin and smoothed with a 5-bin top hat averaged (Veizer et al., 2000). The solid line is the predicted ΔT based on the nominal CRF model above while also taking into account a secular long-term linear contribution. The light dashed line is the residual. The largest residual is at 250 My b.p., where only a few measurements of δ^{18}O exist due to the dearth of fossils subsequent to the largest extinction event in Earth history. The bars at the top represent cool climate modes (icehouses) and the white bars are the warm modes (greenhouses), as established from sedimentological criteria (Frakes and Francis, 1998, Frakes et al., 1992). The lighter shading for the Jurassic-Cretaceous icehouse reflects the fact that true polar ice caps have not been documented for this time interval.

bunched, the fraction is about 100 times smaller, while it is about 5 times larger if the criterion for bunching is a separation of 100 Myr or less). The fraction becomes roughly 6×10^{-5} (or a 4-σ fluctuation), to coincidentally fit the actual period seen in the Iron meteorites.

We see that irrespective of the exact assumptions on the priors, we find a statistically significant result. Also important is the redundancy in the correlations. Namely, there are two independent celestial signals and two independent geological signals all correlating with each other, such that the conclusions do not rest on the validity of any single set of data.

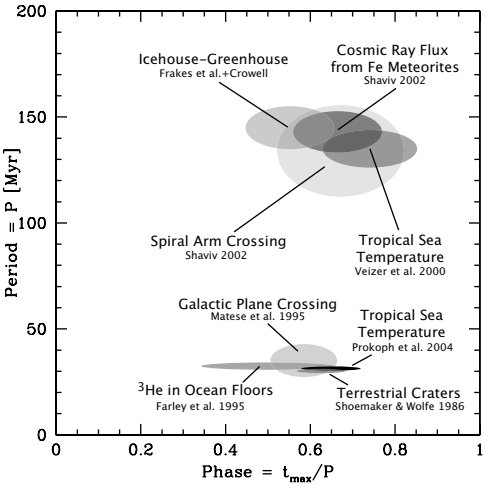

Figure 1.8. The period and phase of various measured signals. The phase is defined as the time (before present) of either observed or predicted maximum warmth, relative to the period. The four signals plotted at the top all have a $\sim$ 145 Myr periodicity. Two signals are extraterrestrial "signals". They have the same periodicity and phase as two independent terrestrial records. Plotted at the bottom are three extraterrestrial signals that are consistent with the observed 32 Myr climatic oscillation. The crater record includes a not very significant periodicity at 31 ± 1 Myr, but it is coincident with other periods.

4.3.3 A possible record of the vertical oscillations. Various spectral analyses of paleoclimate variability have shown that climate may be exhibiting oscillations at different periods. One of these oscillations has a periodicity around $\sim$ 32 Myr, and appears to be more pronounced during the Mesozoic and late Paleozoic (e.g., Prokoph and Veizer, 1999, and references therein). It is of particular interest to us here because it may correspond to a signal formed as a response to the vertical oscillations of the solar system, relative to the galactic plane.

Recently, the δ^{18}O data (Veizer, 1999), with which the Phanerozoic tropical temperature was reconstructed, was expanded such that previous gaps were filled (Prokoph et al., 2004). This allowed analysis of the temperature reconstruction at a higher resolution, with the result that in addition to the large oscillation with a 145 Myr periodicity, the 32 Myr oscillation appears very pronounced over 400 Myr (see fig. 1.9).

Whether or not this oscillation is indeed linked to plane crossing is yet to be proved. Empirically, however, it consistent both in phase and period with the expectation. Irrespectively, the stability of the period indicates that it is most likely of celestial origin.

The physical link to the vertical galactic oscillations is even more interesting to address. We expect CRF variations originating due to the vertical stratification, but under nominal parameters for the CRF/climate effect, the expected signal is at least 2 to 3 times smaller than actually observed (Prokoph et al., 2004). Another possibility is that the Oort cloud is periodically perturbed, and the injected comets later disintegrate and accreted. However, if the dust has the same radiative properties as volcanic ash which is occasionally injected into the stratosphere, the effect is about 10 times smaller than required to explain the observed δ^{18}O oscillations (Prokoph et al., 2004). Interestingly, the ^{3}He based mea-

surements do indicate that the flux of interplanetary dust does vary by a factor of a few, and the three largest peaks do coincide with minimum temperatures of the 32 Myr oscillations (Farley, 1995). If we are underestimating the effect of the dust (e.g., if the particle size is different than volcanic ash, its residence time in stratosphere and its radiative properties will be different), we may be seeing a combined signature of the gravitational tides perturbing the Oort cloud and of a variable CRF.

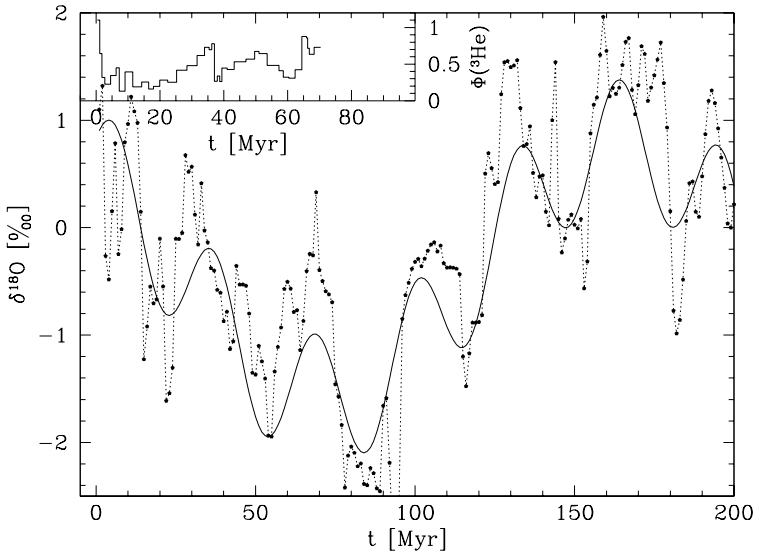

Figure 1.9. Plotted are the tropical ocean δ^{18}O record (which is primarily sensitive to the average temperature—higher δ^{18}O values imply lower temperatures) over the past 200 Myr, and a double oscillation model. The model δ^{18}O (and temperature) is assumed to have a long period oscillation, with a 145 Myr periodicity, and a short period oscillation, with a 32 Myr periodicity (Prokoph et al., 2004). The long periodicity is most likely part of the spiral arm passages. The short periodicity is consistent in both period and phase with the vertical oscillations, perpendicular to the galactic plane. The amplitude of the short period oscillation is, however, somewhat larger than would be expected from just a CRF/climate link. The inset shows the flux of ^{3}He (Farley, 1995, in units of 10^{-12} pcc cm^{-2} kyr^{-1}), which is a proxy of the extraterrestrial dust reaching Earth. The three highest peaks in the dust accretion coincide with minima temperature according to the δ^{18}O reconstruction (but not the fourth peak). These could arise from Oort cloud comets injected into the inner solar system and disintegrating each plane crossing. It could also be a coincidence.

5. Crater record

We have seen that if the Oort cloud is periodically perturbed, then the modulation of the accretion rate of interplanetary dust could be

detected. However, the same periodicity may also manifest itself in record in the terrestrial impact craters.

Shoemaker and Sheomaker, 1993, have argued that extinct comets are more numerous than previously estimated, and concluded the about 50% of the terrestrial craters $\gtrsim$20 km in diameter were due to long and short period comets and that the fraction increases with crater diameter. Moreover, Heisler and Tremaine, 1989, have argued using a Monte Carlo analysis that the null hypothesis of randomness in the cratering record can be ruled out, at the 90% c.l., if the r.m.s. of the dating error is 4 Myr or less. Thus, a periodic cratering signal could exhibit periodicity if larger accurately dated craters are considered.

Shoemaker and Wolfe, 1986, considered 25 young ($\lesssim$220 Myr) accurately dated craters, with a relatively low diameter cutoff of 5 km. They found a significant periodicity of 32 ± 1 Myr, with a last peak at 4 ± 2 Myr. They conclude the the four most recent peaks in the crater rate (at $\approx 2, 32, 65$ and 99 Myr) appear to be too close to the predicted plane crossing events, presumably ruling out more stochastic mechanisms such as Oort cloud perturbation by the gravitational impulses of molecular clouds.

In an improved statistical analysis (Yabushita, 1994), it was argued that the 31 Myr periodicity is significant at the 0.2% level for a 5 km diameter cutoff, and 0.4% level for a 10 km cutoff. Yabushita also compared the 31 Myr period with the 26 Myr period apparent in the extinction record (Raup and Sepkoski, 1984) but did not find any conclusive link.

It is interesting to note that the periodicity and phase found by Shoemaker and Wolfe, 1986, are consistent with the three major peaks in the Farley, 1995, dust accretion data, and the δ^{18}O inferred temperature variations. Thus, craters too may be registering Oort cloud perturbations.

6. Summary

Over long time scales, the three most important causes of change in the environment of the solar system, on times scales of 10^7 yr or longer, are the following:

1 Star formation rate: Over time scales of a few 10^8 yr and longer, the SFR in the solar vicinity varies. The SFR can be reconstructed using stellar clusters (typically on time scales up to several 10^8 yr, since stellar clusters disperse over longer time scales), or using the distribution of individually estimated stellar ages. The various reconstructions reveal elevated rates over the past Eon (with in-

creased activity at ~ 0.3 and ~ 0.7 Gyr), before 2 to 3 Gyr, and before 4 to 5 Gyr. Estimates for the LMC's orbit give perigalactic passages coincident with the above peaks. This is probably not sufficient to prove a cause, but it is interesting to note that the LMC too appears to have had a paucity of star formation after 2 Gyr b.p. During periods of higher star formation activity, more SN produce more cosmic rays, and other cataclysmic events could happen more frequently.

2 Passage through galactic spiral arms: Every ∼145 Myr, the solar system passes through one of the four arms belonging to the outer spiral set. The last passage was of the Saggitarius-Carina arm. Since we are close to the co-rotation radius of a second set (which today happens to coincide with arms of the first set), arms of the second set are traversed very infrequently. Since spiral arms are the main regions of star formation activity in our galaxy, most SNe and subsequent cosmic ray acceleration takes place there. The cosmic ray density is therefore expected to be higher near the arms. Because the ISM is more diverse inside the arms, more effects can take place while crossing them, including for example, passages through a molecular cloud or in the vicinity of massive stars.

3 Oscillations perpendicular to the galactic plane: Since the galactic potential is far from Kerplerian, different perturbations to the circular motion have different periods. In particular, vertical oscillations relative to the galactic plane have a relatively "short" period, estimated at 35 ± 8 Myr (Matese et al., 1995) for example. The relatively large inaccuracy arises because of the uncertainties in the amount of matter, and in particular dark matter, in the Milky Way's disk. The current vertical amplitude is about 100 pc, notably smaller than other objects with the solar system's age. The phase is better known—the last plane crossing took place a few Myr before present.

The above variations in the solar system's environment are more than hypothetical. In fact, very diverse records from different disciplines (other than the astronomical data used to "predict" these variations) registered the above variability. In particular,

1 Iron Meteorites record their exposure to cosmic rays on time scales of $\gtrsim 10^8$ yr and can therefore be used to reconstruct the variations of the CRF. The inconsistency between ^{40}K based exposure ages of individual meteorites and those derived which "short" half-lived radioisotopes, has been long used to show that the CRF over the

past few million years has been higher than the average over the past 1 Gyr. Using a statistical analysis of the Iron meteorites exposure ages, it is possible to reconstruct the actual CRF variations and obtain a clear ~ 145 periodicity in the CRF history. Thus, Iron meteorites recorded our spiral arm passages.

2 ^{3}He in sea floor sedimentation is sensitive to the flux of extraterrestrial dust. Measurement over the past 70 millions years reveal 4 major peaks. The larger 3 have a ~ 33 Myr periodicity and a phase consistent with the vertical oscillations. One plausible explanation is that each plane crossing, the Oort cloud was gravitationally perturbed, more comets where injected into the inner solar system where they disintegrated and accreted as dust. It is unlikely to be variations in accreted ISM dust because its flux relative to solar accreted material is minute. Deeper sea floor excavations may prove or disprove this picture if peaks at ~ 102 Myr and ~ 145 Myr will be detected. Direct reconstruction of the accretion of interstellar dust will soon be available through measurement of ^{244}Pu in sea floor cores, thereby providing a real temporal record of the dusty environment outside the solar system.

3 Paleoclimate Records: A growing body of evidence suggest that climate is sensitive to the amount of tropospheric ionization, governed by the changes in the cosmic ray ionization. Namely, climate proxies could be registering changes in the CRF. The paleoclimate itself can be reconstructed using sedimentation data (e.g., deposits left by glaciers, by evaporating salt lakes, etc.) or using isotopic data (i.e., δ^{18}O in fossils, which is sensitive to the oceanic water temperature and amount of ice-sheets). And indeed, the paleoclimatic data appears to have recorded all the three predicted temperature variations arising from the varying galactic environment. Long term glacial activity on Earth (in the past eon and between 2.2 and 2.7 Gyr before present) correlates with star formation activity. Over the past eon, 7 spiral arm passages, as recoded in the meteoritic data coincide with ice-age epochs on Earth, during which glaciations are present. Last, the δ^{18}O temperature reconstructions reveals a remarkable ~ 32 Myr periodicity over at least 12 cycles. This periodicity is consistent with the vertical oscillations (in particular their phase). If indeed these variations correspond to the vertical oscillations, then an unresolved problem is their amplitude, which is more than twice larger than could be naively expected from the CRF/climate link. One possibility is that we underestimate the vertical stratification of the cosmic ray

flux distribution. Another possibility is that the accreted dust can markably affect climate as well.

References

Alvarez, L. W., Alvarez, W., Asaro, F., and Michel, H. V. (1980). Extraterrestrial cause for the Cretaceous Tertiary extinction. *Science*, 208:1095–1108.

Amaral, L. H. and Lepine, J. R. D. (1997). A self-consistent model of the spiral structure of the galaxy. *Mon. Not. Roy. Astr. Soc.*, 286:885–894.

Aylmer, D., Bonanno, V., Herzog, G. F., Weber, H., Klein, J., and Middleton, R. (1988). ^{26}Al and ^{10}Be production in iron meteorites. *Earth and Plan. Sci. Lett.*, 88:107–118.

Bahcall, J. N. and Bahcall, S. (1985). The sun's motion perpendicular to the galactic plane. *Nature*, 316:706–708.

Barry, D. C. (1988). The chromospheric age dependence of the birthrate, composition, motions, and rotation of late F and G dwarfs within 25 parsecs of the sun. *Astrophys. J.*, 334:436–448.

Beer, J., Mende, W., and Stellmacher, R. (2000). The role of the sun in climate forcing. *Quatenary Science Reviews*, 19:403–415.

Binney, J. and Tremaine, S. (1987). *Galactic dynamics*. Princeton, NJ, Princeton University Press, 747 p.

Blitz, L., Fich, M., and Kulkarni, S. (1983). The new Milky Way. *Science*, 220:1233–1240.

Boella, G., Gervasi, M., Potenza, M. A. C., Rancoita, P. G., and Usoskin, I. (1998). Modulated antiproton fluxes for interstellar production models. *Astroparticle Physics*, 9:261–267.

Boulares, A. and Cox, D. P. (1990). Galactic hydrostatic equilibrium with magnetic tension and cosmic-ray diffusion. *Astrophys. J.*, 365:544–558.

Castagnoli, G. C. and Lal, D. (1980). Solar modulation effects in terrestrial production of carbon 14. *Radiocarbon*, 22:133–158.

Crowell, J. C. (1999). *Pre-Mesozoic ice ages: their bearing on understanding the climate system*, volume 192. Memoir Geological Society of America.

Dame, T. M., Hartmann, D., and Thaddeus, P. (2001). The Milky Way in molecular clouds: A new complete CO survey. *Astrophys. J.*, 547:792–813.

Davis, M., Hut, P., and Muller, R. A. (1984). Extinction of species by periodic comet showers. *Nature*, 308:715–717.

de La Fuente Marcos, R. and de La Fuente Marcos, C. (2004). On the recent star formation history of the Milky Way disk. *New Astronomy*, 9:475–502.

Eddy, J. (1976). The Mounder minimum. *Science*, 192:1189–1202.

Eichkorn, S., Wilhelm, S., Aufmhoff, H., Wohlfrom, K. H., and Arnold, F. (2002). Cosmic ray-induced aerosol formation: first observational evidence from aircraft based ion mass spectrometer measurements in the upper troposphere. *Geophys. Res. Lett.*, 29:10.1029/2002GL015044.

Farley, K. A. (1995). Cenozoic variations in the flux of interplanetary dust recorded by ^{3}He in a deep-sea sediment. *Nature*, 376:153–156.

Ferriere, K. (1998). Global model of the interstellar medium in our galaxy with new constraints on the hot gas component. *Astrophys. J.*, 497:759–776.

Frakes, L. A., Francis, E., and Syktus, J. I. (1992). *Climate modes of the Phanerozoic; the history of the Earth's climate over the past 600 million years*. Cambridge: Cambridge University Press, 1992.

Frakes, L. A. and Francis, J. E. (1998). A guide to Phanerozoic cold polar climates from high-latitude ice rafting in the cretaceous. *Nature*, 333:547–549.

Frisch, P. C. et al. (1999). Dust in the local interstellar wind. *Astrophys. J.*, 525:492–516.

Gardiner, L. T., Sawa, T., and Fujimoto, M. (1994). Numerical simulations of the Magellanic system - part one - orbits of the Magellanic Clouds and the global gas distribution. *Mon. Not. Roy. Astr. Soc.*, 266:567–582.

Gleeson, L. J. and Axford, W. I. (1968). Solar modulation of galactic cosmic rays. *Astrophys. J.*, 154:1011–1026.

Hampel, W. and Schaeffer, O. A. (1979). ^{26}Al in iron meteorites and the constancy of cosmic ray intensity in the past. *Earth Planet. Sci. Lett.*, 42:348–358.

Harrison, R.G. and Aplin, K.L. (2001). Atmospheric condensation nuclei formation and high-energy radiation. *J. Atmos. Solar-Terr. Phys.*, 63:1811–1819.

Heisler, J. and Tremaine, S. (1986). The influence of the galactic tidal field on the Oort comet cloud. *Icarus*, 65:13–26.

Heisler, J. and Tremaine, S. (1989). How dating uncertainties affect the detection of periodicity in extinctions and craters. *Icarus*, 77:213–219.

Heisler, J., Tremaine, S., and Alcock, C. (1987). The frequency and intensity of comet showers from the oort cloud. *Icarus*, 70:269–288.

Hernandez, X., Valls-Gabaud, D., and Gilmore, G. (2000). The recent star formation history of the Hipparcos solar neighbourhood. *Mon. Not. Roy. Astr. Soc.*, 316:605–612.

Herschel, W. (1796). Some remarks on the stability of the light of the sun. *Philosophical Transactions of the Royal Society, London*, page 166.

Hodell, D. A., Brenner, M., Curtis, J. H., and Guilderson, T. (2001). Solar forcing of drought frequency in the Maya lowlands. *Science*, 292:1367–1370.

Hoyle, F. and Wickramasinghe, C. (1978). Comets, ice ages, and ecological catastrophes. *Astrophys. Sp. Sci.*, 53:523–526.

Kasting, J. F. (1993). Earth's early atmosphere. *Science*, 259:920–926.

Kuhn, W. R. and Kasting, J. F. (1983). Effects of increased CO_2 concentrations on surface temperature of the early earth. *Nature*, 301:53–55.

Kyte, F. T. and Wasson, J. T. (1986). Accretion rate of extraterrestrial matter - Iridium deposited 33 to 67 million years ago. *Science*, 232:1225–1229.

Labitzke, K. and van Loon, H. (1992). Association between the 11-year solar cycle and the atmosphere. Part V: Summer. *Journal of Climate*, 5:240–251.

Landgraf, M., Baggaley, W. J., Grün, E., Krüger, H., and Linkert, G. (2000). Aspects of the mass distribution of interstellar dust grains in the solar system from in situ measurements. *J. Geopys. Res.*, 105:10343–10352.

Lassen, K. and Friis-Christensen, E. (1995). Variability of the solar cycle length during the past five centuries and the apparent association with terrestrial climate. *J. Atmos. Terr. Phys.*, 57:835–845.

Lavielle, B., Marti, K., Jeannot, J., Nishiizumi, K., and Caffee, M. (1999). The ^{36}Cl-^{36}Ar-^{40}K-^{41}K records and cosmic ray production rates in iron meteorites. *Earth Planet. Sci. Lett.*, 170:93–104.

Leitch, E. M. and Vasisht, G. (1998). Mass extinctions and the sun's encounters with spiral arms. *New Astronomy*, 3:51–56.

Lin, C. C. and Shu, F. H. (1964). On the spiral structure of disk galaxies. *Astrophys. J.*, 140:646–655.

Lin, D. N. C., Jones, B. F., and Klemola, A. R. (1995). The motion of the Magellanic clouds, origin of the Magellanic Stream, and the mass of the Milky Way. *Astrophys. J.*, 439:652–671.

Loktin, A. V., Matkin, N. V., and Gerasimenko, T. P. (1994). Catalogue of open cluster parameters from UBV-data. *Astronomical and Astrophysical Transactions*, 4:153.

Marsh, N. and Svensmark, H. (2000). Cosmic rays, clouds, and climate. *Space Science Reviews*, 94:215–230.

Matese, J. J. and Whitman, P. G. (1989). The galactic disk tidal field and the nonrandom distribution of observed Oort cloud comets. *Icarus*, 82:389–401.

Matese, J. J., Whitman, P. G., Innanen, K. A., and Valtonen, M. J. (1995). Periodic modulation of the Oort cloud comet flux by the adiabatically changing galactic tide. *Icarus*, 116:255–268.

Naoz, S. and Shaviv, N. J. (2004). Open star clusters and the Milky Way's spiral arm dynamics. Submitted to Astrophys. J.

Napier, W. M. and Clube, S. V. M. (1979). A theory of terrestrial catastrophism. *Nature*, 282:455–459.

Neff, U., Burns, S. J., Mangnini, A., Mudelsee, M., Fleitmann, D., and Matter, A. (2001). Strong coherence between solar variability and the monsoon in Oman between 9 and 6 kyr ago. *Nature*, 411:290–293.

Ney, E. P. (1959). Cosmic radiation and weather. *Nature*, 183:451.

Palle Bago, E. and Butler, J. (2000). The influence of cosmic terrestrial clouds and global warming. *Astronomy & Geophysics*, 41:18–22.

Palous, J., Ruprecht, J., Dluzhnevskaia, O. B., and Piskunov, T. (1977). Places of formation of 24 open clusters. *Astron. Astrophys.*, 61:27–37.

Paul, M. et al. (2001). Experimental limit to interstellar ^{244}Pu abundance. *Astrophys. J.*, 558:L133–L135.

Pavlov, A. A., Kasting, J. F., Brown, L. L., Rages, K. A., and Freedman, R. (2000). Greenhouse warming by CH_4 in the atmosphere of early earth. *J. Geophys. Res.-Plan.*, 105 (E5):11981–11990.

Pollack, J. B. (1991). Kuiper prize lecture - present and past climates of the terrestrial planets. *Icarus*, 91:173–198.

Prokoph, A., Shaviv, N. J., and Veizer, J. (2004). A 32 Ma climate periodicity and its possible celestial link. Submitted to Geology.

Prokoph, A. and Veizer, J. (1999). Trends, cycles and nonstationarities in isotope signals of Phanerozoic seawater. *Chem. Geology*, 161:225–240.

Rampino, M. R. and Stothers, R. B. (1984). Terrestrial mass extinctions, cometary impacts and the sun's motion perpendicular to the galactic plane. *Nature*, 308:709–712.

Rampino, M. R. and Stothers, R. B. (1986). Geologic periodicities and the galaxy. *The Galaxy and the Solar System*, pages 241–259.

Raup, D. M. and Sepkoski, J. J. (1984). Periodicity of extinction in the geologic past. *Proc. Natl. Acad. Sci.*, 81:801–805.

Ready, R. C. (1987). Nuclide production by primary-ray protons. *J. Geophys. Res. Supp.*, 92:E697–E702.

Rocha-Pinto, H. J., Scalo, J., Maciel, W. J., and Flynn, C. (2000). Chemical enrichment and star formation in the Milky Way disk. II. Star formation history. *Astron. Astrophys.*, 358:869–885.

Rye, R., Kuo, P. H., and Holland, H. D. (1995). Atmospheric carbon dioxide concentrations before 2.2 billion years ago. *Nature*, 378:603–605.

Sagan, C. and Chyba, C. (1997). The early faint sun paradox: Organic shielding of UV-labile greenhouse gases. *Science*, 276:1217–1221.

Sagan, C. and Mullen, G. (1972). Earth and mars - evolution of atmospheres and surface temperatures. *Science*, 177:52.

Scalo, J. M. (1987). The initial mass function, starbursts, and the Milky Way. In *Starbursts and Galaxy Evolution*, pages 445–465.

Schaeffer, O. A., Nagel, K., Fechtig, H., and Neukum, G. (1981). Space erosion of meteorites and the secular variation of cosmic rays over 10^9 years. *Planet. Sp. Sci.*, 29:1109–1118.

Shaviv, N. J. (2002). Cosmic ray diffusion from the galactic spiral arms, iron meteorites, and a possible climatic connection. *Physical Review Letters*, 89(5):051102.

Shaviv, N. J. (2003a). The spiral structure of the Milky Way, cosmic rays, and ice age epochs on earth. *New Astronomy*, 8:39–77.

Shaviv, N. J. (2003b). Toward a solution to the early faint sun paradox: A lower cosmic ray flux from a stronger solar wind. *J. Geophys. Res.–Space Physics*, 108:1437.

Shaviv, N. J. (2004). On climate response to changes in the cosmic ray flux and radiative budget. submitted to J. Geophys. Res.–Atmos.

Shaviv, N. J. and Veizer, J. (2003). Celestial driver of Phanerozoic climate? *GSA Today*, 13(7):4–10.

Shoemaker, E. M. and Sheomaker, C. S. (1993). The flux of periodic coments near earth. In *Asteroids, Comets, Meteors*. IAU Symposium 160, abstract 270.

Shoemaker, E. M. and Wolfe, R. F. (1986). Mass extinctions, crater ages and comet showers. *The Galaxy and the Solar System*, pages 338–386.

Soon, W. H., Posmentier, E. S., and Baliunas, S. L. (1996). Inference of solar irradiance variability from terrestrial temperature changes, 1880-1993: an astrophysical application of the sun-climate connection. *Astrophys. J.*, 472:891.

Soon, W. H., Posmentier, E. S., and Baliunas, S. L. (2000). Climate hypersensitivity to solar forcing? *Annales Geophysicae*, 18:583–588.

Stothers, R. B. (1998). Galactic disc dark matter, terrestrial impact cratering and the law of large numbers. *Mon. Not. Roy. Astr. Soc.*, 300:1098–1104.

Svensmark, H. (1998). Influence of cosmic rays on earth's climate. *Physical Review Letters*, 81:5027–5030.

Svensmark, H. (2000). Cosmic rays and earth's climate. *Space Science Reviews*, 93:175–185.

Svensmark, H. and Friis-Christensen, E. (1997). Variation of cosmic ray flux and global cloud coverage–a missing link in solar-climate relationships. *J. Atmos. Terr. Phys.*, 59:1225–1232.

Talbot, R. J. and Newman, M. J. (1977). Encounters between stars and dense interstellar clouds. *Astrophys. J. Supp.*, 34:295–308.

Taylor, J. H. and Cordes, J. M. (1993). Pulsar distances and the galactic distribution of free electrons. *Astrophys. J.*, 411:674–684.

Torbett, M. V. (1986). Injection of Oort cloud comets to the inner solar system by galactic tidal fields. *Mon. Not. Roy. Astr. Soc.*, 223:885–895.

Usoskin, I. G., Marsh, N., Kovaltsov, G. A., Mursula, K., and Gladysheva, O. G. (2004). Latitudinal dependence of low cloud amount on cosmic ray induced ionization. *Geopys. Res. Let.*, 31:6109.

Veizer, J., Godderis, Y., and Francois, L. M. (2000). Evidence for decoupling of atmospheric CO_2 and global climate during the Phanerozoic eon. *Nature*, 408:698.

Veizer, J. et al. (1999). $^{87}Sr/^{86}Sr$, ^{13}C and ^{18}O evolution of Phanerozoic seawater. *Chemical Geology*, 161:59–88.

Wielen, R. (1977). The diffusion of stellar orbits derived from the observed age-depen dence of the velocity dispersion. *Astron. Astrophys.*, 60:263–275.

Wood, B. E., Müller, H., Zank, G. P., and Linsky, J. L. (2002). Measured mass-loss rates of solar-like stars as a function of age and activity. *Astrophys. J.*, 574:412–425.

Yabushita, S. (1994). Are periodicities in crater formations and mass extinctions related? *Earth Moon and Planets*, 64:207–216.

Yu, F. (2002). Altitude variations of cosmic ray induced production of aerosols: Implications for global cloudiness and climate. *J. Geophys. Res.*, 248:248.